FRFT-based Parameter Estimation of Time-varying Wideband Underwater Acoustic Multipath Channels*

Yanbo Zhao, Hua Yu† , Gang Wei, Fei Ji, Fangjiong Chen and Jun Zhang
School of Electronic and Information Engineering
South China University of Technology
Guangzhou, 510640 China
yuhua@scut.edu.cn

ABSTRACT

The time-varying property and wideband nature are considered as the most difficult challenges of the underwater acoustic channels. Due to the low propagation speed of the sound, the relative motion between the transmitter and receiver can result in serious Doppler effect. Even if both of the platforms stay still, the multipath signals along different eigenrays vary in angles of arrival, hence the radial velocities. Such Doppler velocities brings different time compressions or dilations to the multipath signals. In addition, as the signal bandwidth is usually comparable to the center frequency, it is more appropriate for the underwater acoustic channels to be modeled as wideband channels. In this paper, the parameter estimation of the wideband time-varying underwater acoustic channels is investigated. Linear frequency modulation signals are used as the training sequences, and the fractional Fourier transform is the key of the estimation algorithm. The communication scenario, with a fixed transmitter and a moving receiver, is built by the Bellhop software. The generated channel impulse response shows obvious time-varying property, as well as sparsity, in the multipath amplitudes and delays. The estimation result recovers the channel impulse response very well, thus confirms the effectiveness of the proposed method.

Keywords

wideband underwater acoustic channel, delay-scale spreading function, channel estimation, fractional Fourier tranform, sparse multipath channel.

*This work was supported in part by the National Natural Science Foundation of China (61431005, 61372081, 61271209, 61372083), Key Grant Project of Chinese Ministry of Education (313021), Key Grant Project of Natural Science Foundation of Guangdong Province, China (2014A030311034), and Science and Technology Planning Project of Guangdong Province, China.

†Corresponding author.

WUWNET '15, October 22-24 2015, Washington DC, USA

http://dx.doi.org/10.1145/2831296.2831304

1. INTRODUCTION

The underwater acoustic (UWA) channels are characterized by time-frequency double dispersion and considered as perhaps the most complicated wireless channels [1–4]. The low propagation speed of acoustic wave and multiple scatterers result in large multipath delay spread, and such multipath propagation leads the UWA channels to perform severe multiplicative effects on the transmit signal in the frequency domain. Hence, the UWA channels are frequency-selective. In addition, the relative motion can cause the Doppler effect, which leads to time-varying (TV) multiplicative effects on the transmit signal in the time domain, so the UWA channels are also time-selective.

Since angles of arrival and the relative velocities linked with the received multipath components are typically different, the individual components will be stretched or compressed in time. In frequency domain, accordingly, the spectrums will be stretched compressed or stretched by Doppler scaling factors [5]. In narrowband systems, such Doppler scales can be approximated as Doppler shifts. However, more and more attention has been paid to the wideband nature of the UWA channels in literatures, e.g. [5–10]. For many acoustic signals, the fractional bandwidth (ratio of bandwidth over carrier frequency) and the time-bandwidth product are usually so large that the narrowband condition does not hold. Thus, to describe the Doppler effect of the UWA channels more suitably, the Doppler scaling factor should be employed.

There are several factors which produce the relative motion between the transmitter and the receiver for communication application, or between the sonar and the target for detection application. The active factor is the vehicular motion of the platforms [7], and the passive factors includes the reflections from the moving surface [5] [7] [11], unintentional ocean internal waves [12], and the varying depth(pressure, temperature and salinity)-dependent sound speed [13]. These types of motion will together generate a relative radial velocity, which will influence the Doppler scaling factor of each multipath. The Doppler spread will seriously affect the reliability of communication performance.

For UWA communication applications, to capture the original information accurately, parameter estimation for such multiscale-multilag (MSML) channels is required. Since the scaling changes involve resampling process at the receiver, most existing channel estimation methods only consider and compensate one dominant scale factor [14–16]. Although it simplifies the receiver structure, such scale compensation

mechanism leaves residual sampling errors for other scaled components, and ignores the potential diversity which could be exploited in a time-scale channel characterization to increase communication performance [17]. The channel impulse response (CIR) is always the object of the parameter estimation, since it has important roles in the target probing, source localization, timing synchronization, and the channel equalization. Training-based estimation methods are commonly used in wireless communication applications. The frequently used training sequences include the m-sequence [18], Zadoff−Chu sequence [19], etc. For wideband channels, the frequency modulation (FM) signal is good choices to be the channel training sequences because it has large time-bandwidth product and good autocorrelation characteristic [6] [7]. In the field of target detection, the linear frequency modulation (LFM) signal and the hyperbolic frequency modulation (HFM) signal are frequently used [20]. Although the HFM signal is Doppler-invariant, the Doppler scaling will cause a time shift to its main pulse of the matched filter output. By comparison, the LFM signal can be compressed by the matched filter and forms a narrower main pulse than the HFM does, but it is not Doppler-invariant [21]. When a Doppler scaling change occurs, the main pulse will be broadened and sidelobe levels will be increased.

In previous research on the parameter estimation of the MSML UWA channels, a matched filter bank scheme is proposed in [8], and the matching pursuit (MP) decomposition algorithm is used in [9]. Essentially, both of these two methods calculate the correlation between the received signal and the scaled-delayed versions of the original training sequence. The Doppler scale spread and delay spread should be known beforehand for both of these methods. When the Doppler scale spread is large and fine time-scale resolution is required, a huge number of filters are needed for the method in [8], while a super large signal dictionary should be built for the MP decomposition algorithm in [9].

The fractional Fourier transform (FRFT) is a generalization of the classical Fourier transform, and can be interpreted as a rotation in the time-frequency plane [22, 23]. In the FRFT domain, an LFM signal can be represented as an impulse at an appropriate time-frequency rotation angle. In [24], the FRFT is used to compensate a known single Doppler scale of the LFM echoes. For the LFM signal with an unknown scale factor, the key to estimate the scale factor is to find the optimal fractional order of the signal's FRFT, or the rotation angle at which the transformed signal reaches a maximum amplitude and forms an impulse. A coarse-to-fine method is proposed to estimate the compact fractional domain in [25]. However, accurate estimation methods for the MSML UWA channels still lack of further study. In this paper, selecting the LFM signal as training sequence, an FRFT-based parameter estimation method for the wideband time-varying UWA channel is proposed. It can obtain the MSML coefficients without knowing the Doppler scale spread beforehand nor any resampling operation, and can safely ignore the time-varying depth-dependent sound speed and other relative motion types mentioned above. The CIR estimation performance of the proposed method exceeds those of the matched filter with single resampling rate [16] and MP decomposition method [9].

The remainder of this paper is organized as follows. Section II reviews the system model, and briefly introduces the FRFT. In Section III, an efficient and accurate FRFT-based parameter estimation method for the wideband time-varying UWA channel is proposed. Computer simulation is given in Section IV, and finally conclusions are drawn in Section V.

2. SYSTEM MODEL

2.1 Wideband TV UWA channel model

Assuming there are L dominant multipaths, the time-varying UWA CIR is defined as [15] [16]

$$h\left(t,\tau\right)=\sum_{l=1}^{L}A_l\left(t\right)\delta\left(\tau-\tau_l\left(t\right)\right) \tag{1}$$

where $A_l\left(t\right)$ and $\tau_l\left(t\right)$ denote the time varying l-th path delay and amplitude, respectively. The time variation of the path delay τ_l can be approximated to change linearly with t as

$$\tau_l\left(t\right)=\tau_l-\left(\alpha_l-1\right)t \tag{2}$$

where $\alpha_l\in\mathbb{R}$ denotes the Doppler scale of the l-th path, and is directly related to the radial velocity v_l of the scatterer and the velocity c of the signal in the propagation medium according to the relationship $\alpha_l=(c-v_l)/(c+v_l)$. Further, the path amplitudes can be assumed constant $A_l(t)\approx A_l$ over the duration of the signal transmission, since the channel coherence time is usually on the order of seconds [14]. Then a path-based channel model is given as

$$h\left(t,\tau\right)=\sum_{l=1}^{L}A_l\delta\Big(\tau-\Big(\tau_l-\left(\alpha_l-1\right)t\Big)\Big) \tag{3}$$

This channel is the so-called MSML channels if the Doppler scales and path delays can be distinguished from each other. Denoting the transmitted signal as $s(t)$, we have the received signal as

$$\begin{aligned} r\left(t\right) &= \int_{-\infty}^{\infty}h\left(t,\tau\right)s\left(t-\tau\right)d\tau+w(t) \\ &= \sum_{l=1}^{L}A_l s\big(\alpha_l t-\tau_l\big)+w(t) \end{aligned} \tag{4}$$

where $w(t)$ denotes the additive noise.

In some other places, the effect of the wideband channel on the transmitted signal can also be described by the delay-scale spreading function (DSSF), which is a continuous function defined in the delay-scale plane [5] [10] [17]. The DSSF can be represented as

$$F_H\left(\alpha,\tau\right)=\sum_{m=1}^{\mathcal{M}}\sum_{n=0}^{\mathcal{N}}A_{m,n}^{H}\delta\left(\alpha-\alpha_m\right)\delta\left(\tau-\tau_n\right) \tag{5}$$

where $\alpha_m=\alpha_{\min}+m\Delta\alpha$, $\tau_n=n\Delta\tau$, $\mathcal{M}=(\alpha_{\max}-\alpha_{\min})/\Delta\alpha$, $\mathcal{N}=\tau_{\max}/\Delta\tau$, with $\alpha_{\min}$, $\alpha_{\max}$, $\tau_{\max}$, $\Delta\alpha$ and $\Delta\tau$ denote the minimum Doppler scale, maximum Doppler scale, maximum delay, the uniform scale sampling interval and delay sampling interval, respectively. $A_{m,n}^{H}$ is the sampling amplitude of the (m,n)-th grid of the discretized DSSF.

2.2 LFM Signal as the Training Sequence

We consider an LFM signal defined on the passband as the channel training sequence $s(t)$, which is

$$s\left(t\right)=\mathrm{Re}\Big[\mathrm{rect}\left(t\right)\exp\left(j\left(2\pi f_0 t+\pi k t^2+\varphi_0\right)\right)\Big] \tag{6}$$

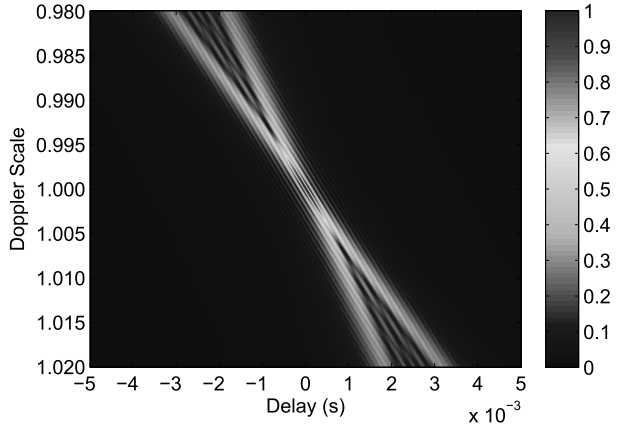

Figure 1: The WAAF of an LFM signal over the Doppler scale range $\alpha \in [0.98, 1.02]$ and the delay range $\tau \in [-5, 5] \times 10^{-3}$s.

where f_0, k and φ_0 are the starting frequency, modulation slope and initial phase, respectively. The stopping frequency is $f_1 = f_0 + kT$, where T is the duration of the signal. The function rect(t) denotes the normalized rectangular window, i.e. rect$(t) = 1/T$ for $t \in [0, T]$ and zero otherwise.

For the LFM signal, if there is not any relative motion, the output of the matched filter at the receiver forms a series of pulses which space corresponding to the multipath delays. When Doppler scales exist due to the relative motion, the correlation pulses could be severely broaden. Such mismatch can be explained and analyzed by the wideband ambiguity function (WAF), which is a function defined by the parameters α and τ. The wideband auto ambiguity function (WAAF) [26] of $s(t)$ is

$$WB_{ss}(\alpha, \tau) = \sqrt{|\alpha|} \int_{-\infty}^{\infty} s(t) s^* \left(\alpha \left(t - \tau\right)\right) dt \tag{7}$$

For any probe signal $s(t)$, its WAAF magnitude reaches a maximum at $(\alpha, \tau) = (1, 0)$. The WAAF, over a range of interest in the delay-scale plane, of an LFM signal is illustrated as Fig. 1. Along with the scale factor changes away from 1, the main pulse of the correlation output is broaden along the delay axis, and the magnitude is weakened.

When the scale factors of the received multipath signals are identical but not equal to 1, a good time-delay correlation output can be obtained by resampling the received signal with the identical scale factor. However, if the scale factors are different with each other, the output of the time-delay correlation, with a single resampling factor, will be blurred by the WAAFs of other multicomponents. In this case, a single resampling factor is not particularly helpful.

2.3 FRFT of the LFM signals

The FRFT of a function $x(t)$, with a fractional order p and a rotation angle $\phi = p\pi/2$, is defined as [22] [23] [27]

$$F^p x = X_\phi \left(u\right) = \int_{-\infty}^{\infty} x \left(t\right) K_\phi \left(t, u\right) dt \tag{8}$$

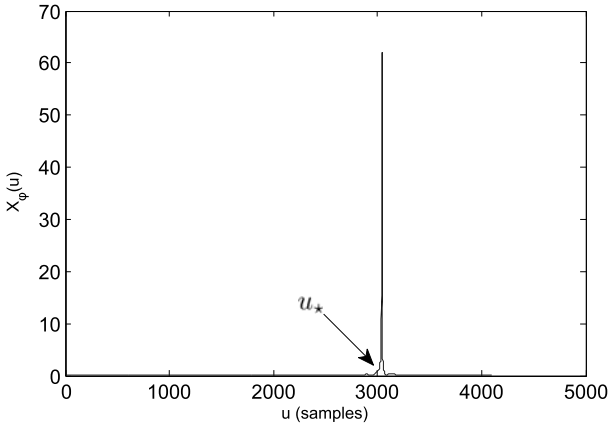

Figure 2: The discrete FRFT of a sampled LFM signal at the ORA $\phi_\star$. The LFM signal, with duration 50ms, sweeps the frequency from 5KHz to 15KHz, and is sampled as a sequence with length 4096. Its discrete FRFT, $X_{\phi_\star}(u)$, is a complex vector with the same length, and the magnitude peaks at $u_\star$.

where $K_\phi(t, u)$ is the transformation kernel, which is defined as

$$K_\phi \left(t, u\right) = \begin{cases} A_\phi \exp\left(j \frac{t^2 + u^2}{2} \cot\phi - jut \csc\phi\right), \text{for } \phi \neq n\pi \\ \delta\left(t - u\right), \text{ for } \phi = 2n\pi \\ \delta\left(t + u\right), \text{ for } \phi = (2n \pm 1)\pi \end{cases}$$

where the complex amplitude factor $A_\phi = \sqrt{\frac{1 - j\cot\phi}{2\pi}}$.

For an LFM signal, there exists an optimal rotation angle (ORA) $\phi_\star$, which gathers the LFM signal energy at $u_\star$. The $X_{\phi_\star}(u)$ forms an impulse function in the FRFT domain, and the maximum value appears as $X_{\phi_\star}(u_\star)$, as shown in Fig.2. The relationship between the ORA and the LFM signal modulation slope is given as [28]

$$k = -\cot\left(\phi_\star\right). \tag{9}$$

3. FRFT-BASED PARAMETER ESTIMATION

3.1 Single Path Channel

When a complex channel attenuation A, a temporal scaling α and a delay τ happen to the LFM signal, the passband received signal is

$$\begin{aligned} r(t) =& \ \mathrm{Re}[A] s\left(\alpha\left(t - \tau\right)\right) - \mathrm{Im}[A] s^+\left(\alpha\left(t - \tau\right)\right) \\ =& \ \mathrm{Re}\Big[A \cdot \mathrm{rect}\left(\alpha\left(t - \tau\right)\right) \exp\left(j\left(2\pi f_0' t + \pi k' t^2 + \varphi_0'\right)\right)\Big] \end{aligned} \tag{10}$$

with

$$\begin{cases} f_0' &= \alpha f_0 - k\alpha^2 \tau \\ k' &= k\alpha^2 \\ \varphi_0' &= \pi k \alpha^2 \tau^2 - 2\pi f_0 \alpha \tau + \varphi_0 \end{cases} \tag{11}$$

where $s^+ = \mathcal{H}(s)$ is the Hilbert transform of $s(t)$.

We can see that the received signal $r(t)$ is still an LFM signal, but the modulation slope changes to $k' = k\alpha^2$.

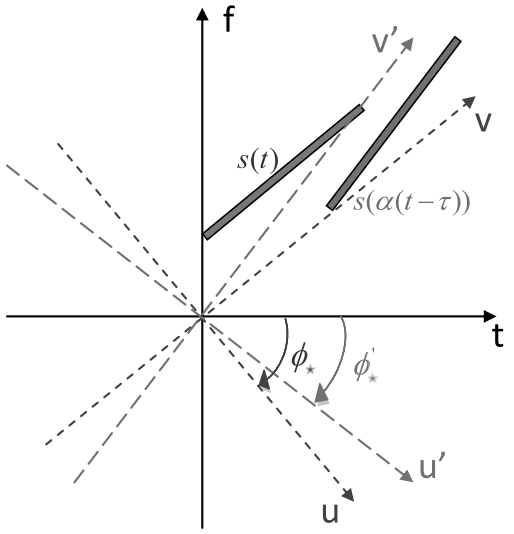

Figure 3: FRFTs of $s(t)$ and $s(\alpha(t-\tau))$. For a LFM signal, there exists an ORA $\phi_\star$, which gathers the signal energy at a certain value on the rotated u-axis, see the dense dotted frame of axes in blue color. Once a time delay and a Doppler scale happen, the ORA switches to $\phi'_\star$, and the signal forms a new impulse function in the u'-v' FRFT domain, see the loose dotted frame of axes in red color.

Accordingly, the transformed LFM signal forms an impulse function at a new ORA $\phi'_\star$, as shown in Fig.3. Combining (9) and (11), we have the following relationship

$$k\widehat{\alpha}^2 = k' = -\cot\left(\phi'_\star\right) \tag{12}$$

Hence, once the degree of the new ORA $\phi'_\star$ is known, the scaling change estimate, $\widehat{\alpha}$, can be obtained since the slope k is known beforehand at the receiver. Then the time delay τ and attenuation A can be estimated through search for the peak of the correlation between $r(t)$ and $s_{\widehat{\alpha}}(t)$, where $s_{\widehat{\alpha}}(t)$ is the resampled $s(t)$ with $\widehat{\alpha}$ as the resampling factor.

Searching for the ORA $\phi'_\star$ in (12) needs many times FRFT computations and comparisons to be done. In [29], a fast digital computation of the FRFT is given. It reduces any fractional order to a general interval $(0.5, 1.5)$. Like FFT, this fast computational algorithm gives samples of the continuous time FRFT of a signal in terms of the same amount of samples of the original signal. Assuming a discrete LFM has N samples under the sampling rate f_s, the frequency resolution $\Delta f = f_s/N$ and the time resolution is $\Delta t = 1/f_s$. According to [28], the modulation slope of the sampled LFM signal is

$$k = -\frac{\Delta f}{\Delta t}\cot\left(\phi_\star\right) = -\frac{f_s^2}{N}\cot\left(\phi_\star\right) \tag{13}$$

Since the LFM signal forms an impulse at the ORA, searching for the ORA is equivalent to scanning the fractional Fourier amplitude spectrum for the maximum value. We use a coarse-to-fine scanning method proposed in [25], which can iteratively calculate the ORA corresponding the the maximum FRFT value. Since such coarse-to-fine scanning requires dozens times of FRFT operations and the fast discrete FRFT only requires $O(N\log N)$ computation [29], the computational complexity of the scanning can be low enough.

3.2 Multipath Channels

In this part, we propose an iterative matching algorithm to estimate the parameters for the MSML channels. For each multicomponent, the estimation is a planar searching process in the scale-delay plane.

Assuming that the analytic signal vector of the transmitted LFM sequence is $\mathbf{s}_{N\times 1}$ and the real received signal vector is $\mathbf{r}_{N_r\times 1}$, first we generate the analytic signal $\mathbf{r}_e = \mathbf{r} + j\cdot\text{Hilbert}(\mathbf{r})$ and denote is as the residual signal. Scan the FRFT domain to obtain the ORA of the entire signal $\mathbf{r}_e$, denoted as ϕ', hence obtain a crude scale factor estimate of the most dominant path

$$\widehat{\alpha} = \sqrt{-\cot\left(\phi'_\star\right) f_s^2/\left(kN_r\right)} \tag{14}$$

Secondly, generate the scaled signal vector $\mathbf{s}_{\widehat{\alpha}}$ with $\widehat{\alpha}$ as the resampling factor, and find the delay index, denoted as d, by operating a cross correlation between $\mathbf{s}_{\widehat{\alpha}}$ and $\mathbf{r}_e$, i.e.

$$d = \max_n \left|\sum_m \mathbf{r}_e[m]\mathbf{s}^*_{\widehat{\alpha}}[m+n]\right| \tag{15}$$

Next, rescan the FRFT domain to obtain the ORA of the partitioned signal $\mathbf{r}_e[d : d+N_i-1]$, where $N_i = \lceil\widehat{\alpha}N\rceil$ is the length of $\mathbf{s}_{\widehat{\alpha}}$. Denote the new ORA as $\phi''_\star$, we have the refined scale estimate

$$\widehat{\alpha}' = \sqrt{-\cot\left(\phi''_\star\right) f_s^2/\left(kN_i\right)} \tag{16}$$

Due to different scanning length, the two estimates $\widehat{\alpha}$ and $\widehat{\alpha}'$ may be different, so we generate a new scaled signal vector and repeat (15) and (16) until the scale estimate does not change anymore. This operation makes the width of the FRFT window dynamically change to adjust the length of the scaled multipath signal, and makes the algorithm return finer estimates of the actual parameters.

Once the scale estimate $\widehat{\alpha}$ stabilizes, the delay and amplitude of the related path can be computed by

$$\widehat{\tau} = d/f_s \tag{17}$$

$$\widehat{A} = \sum_m \mathbf{r}_e[m]\mathbf{s}^*_{\widehat{\alpha}}[m+d]/\|\mathbf{s}_{\widehat{\alpha}}\|_2^2 \tag{18}$$

Finally, update the received signal vector by removing $\mathbf{s}_{\widehat{\alpha}}$

$$\mathbf{r}_e[d : d+N_i-1] \leftarrow \mathbf{r}_e[d : d+N_i-1] - \widehat{A}\mathbf{s}_{\widehat{\alpha}} \tag{19}$$

Then the multicomponent with the highest energy is eliminated from the residual signal.

The parameters of the second most dominant path will be estimated in the same way with the updated $\mathbf{r}_e$. The iteration stops when the number of estimated paths reach a set number, or the ratio of the signal energy to the residual energy reaches the SNR, if known.

The simple structure of the receiver, which using the above proposed algorithm, is a noteworthy advantage. As mentioned in Section 1, the matched filter bank scheme [8] requires multiple filters and multiple sampling rates, of which the number controls the resolution in both the scale and time domain. While the MP decomposition method [9] requires a complete signal-transformed dictionary to be built in advance, whose atoms should cover all possible combinations of the discrete delays and scales. Unlike these methods,

the receiver structure using the proposed algorithm does not need extra hardware overhead or huge signal dictionaries. In addition, other information, such as the vehicle speed and the Doppler scale spread, is not required beforehand since the ORA scanning process can rapidly figure out the scale factor in the whole range for each path.

4. SIMULATION RESULTS

In this section, we evaluate the performance of the proposed FRFT-based parameter estimation algorithm. In the first part, a simple sparse MSML channel is artificially created, and the accuracy of the estimation is quantitatively analyzed. In the second part, time-varying channels for a moving receiver scenario are generated by the BELLHOP software. The time-varying CIR over a period of one minute is estimated by using the proposed method.

4.1 Simple Sparse Multipath Channels

First, we assign the parameters of the transmitted LFM training signal. The bandwidth and time duration are set to be $B = 10$KHz and $T = 50$ms, thus the modulation slope is $k = B/T = 2 \times 10^5$. The starting frequency, stopping frequency and initial phase are $f_0 = 5$KHz, $f_1 = 15$KHz, and $\varphi_0 = 0$, respectively. To obtain a fine scale resolution, the sampling rate f_s is set 8 times of the bandwidth. Second, we hypothesize an sparse MSML channel based on the following assumptions:

1) only 8 multipaths are dominant in energy;

2) all the multipaths are time-compressed and the scale factors are uniformly distributed within $\alpha \in [1, 1.02]$, with an accuracy to three decimal places (Note that the maximum scale 1.02 corresponds to a relative velocity about 30 knots, which is relatively high for underwater movement);

3) all the multipaths arrive at the receiver within one signal duration T (significantly overlap case), and the time delays follow uniformly distribution.

With the generated parameters subjected to these assumptions, the received signal can be obtained by using (4). Next we quantitatively analyze the proposed method accuracy from the performance of the power delay profile estimation and the Doppler scale estimation.

4.1.1 Power Delay Profile (PDP)

The PDP contains information about how much power arrives at the receiver with a particular delay, irrespective of possible Doppler scales. It can be obtained by integrating the DSSF (5) over the scale dimension, and also can be obtained from the complex CIR as

$$P_h(\tau) = \lim_{T\to\infty} \frac{1}{2T} \int_{-T}^{T} |h(t,\tau)|^2 \, dt \tag{20}$$

We use the normalized mean squared error (NMSE) as the performance indicator of the PDP estimation, given as

$$\mathrm{NMSE}_{\mathrm{P_h}} = \frac{\int_{-\infty}^{\infty} \left|\widehat{P}_h(\tau) - P_h(\tau)\right|^2 d\tau}{\int_{-\infty}^{\infty} |P_h(\tau)|^2 \, d\tau} \tag{21}$$

where $\widehat{P}_h(\tau)$ is the estimate of original channel PDP $P_h(\tau)$.

As a comparison, the performance of the single resampling method [16] and the MP decomposition method [9] are also evaluated. For the training sequences of the MP decomposition method, the LFM sequence, m-sequence, and

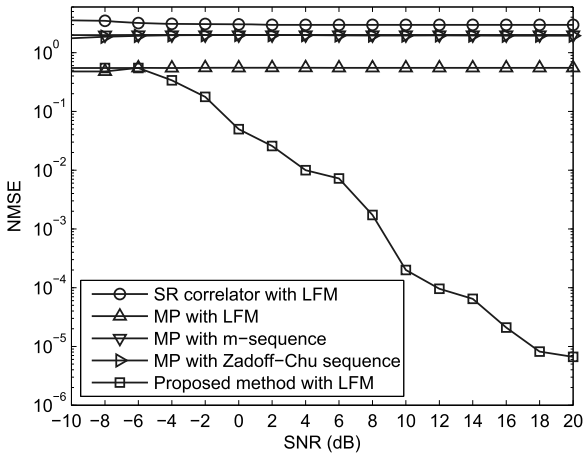

Figure 4: NMSEs of the estimated PDP versus SNR

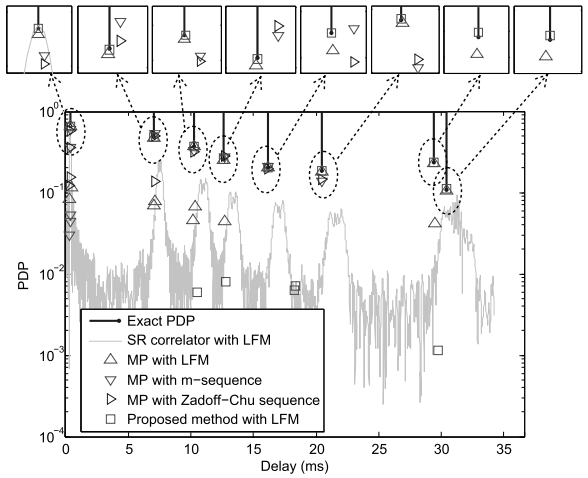

Figure 5: PDP estimates at SNR=20dB (one trial)

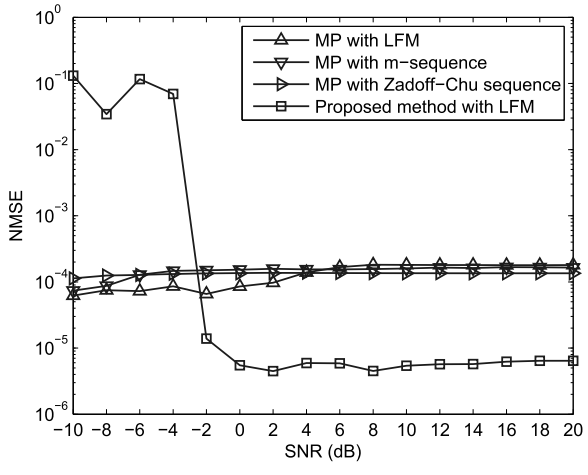

Figure 6: NMSEs of the scale factor estimates of the dominant multipaths versus SNR

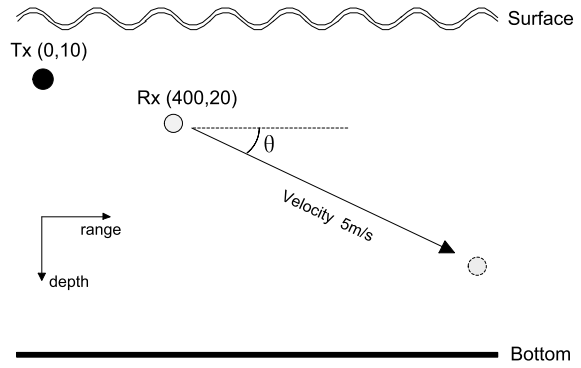

Figure 7: A scenario with a stationary transmitter and a moving receiver.

Zadoff−Chu sequence are simulated respectively. The NMSE is averaged over the results of 200 trials for each estimation method. It can be seen that the proposed method outperforms the others from the NMSE results, which are drawn in Fig.4. More clearly, the PDP NMSEs at SNR=20dB in one trial is illustrated in Fig.5. The amplitudes and delay positions, estimated by the proposed method, are closer to the original channel. Although some redundant estimates exist, the values are so tiny that can be ignored.

4.1.2 Doppler Scale Factor

Since the Doppler scale factor is involved in the parameter estimation, its estimation accuracy should be investigated. Also, we consider the NMSEs of the scale factor estimates of the dominant multipaths as the indicator, i.e.

$$\mathrm{NMSE}_{\alpha} = \frac{\sum_{l=1}^{L} |\widehat{\alpha}_l - \alpha_l|^2}{\sum_{l=1}^{L} |\alpha_l|^2} \tag{22}$$

and show the results in Fig.6. The proposed method obtains more accurate scale estimates than MP-based method when SNR surpasses −2dB, while the MP-based method is barely affected by the noise.

4.2 TV-CIR Generated by BELLHOP

In this part of simulation, we use the Bellhop software to generate a scenario with a moving receiver, and test the proposed method in the time-varying channel. The scenario is illustrated in Fig.7. We assume the maximum depth of water is 100m, and use the coordinates (r, z) to denote the position of horizontal range r and depth z. The transmitter is stationary at $(0, 10)$, while the receiver at $(400, 20)$ starts moving away at velocity 5m/s with a declination angle $\theta = 0.05$ from the horizontal line. Since the depth of the receiver changes with time, we define the sound speed profile as shown in Fig.8. For the receiver at a specific position, the Bellhop output data contains the amplitude-delay information, and the scale-delay information can be obtained according to [30]. Considering the surface is silence, i.e., there is no surface motion, the amplitude and scale versus path delay at the beginning position $(400, 20)$ is shown in Fig.9. As the receiver position changes, we draw the time-varying CIR over 240s in Fig.10.

The LFM signal, with duration $T = 20$ms and spans the frequency from 5KHz to 10KHz, is sent every other second.

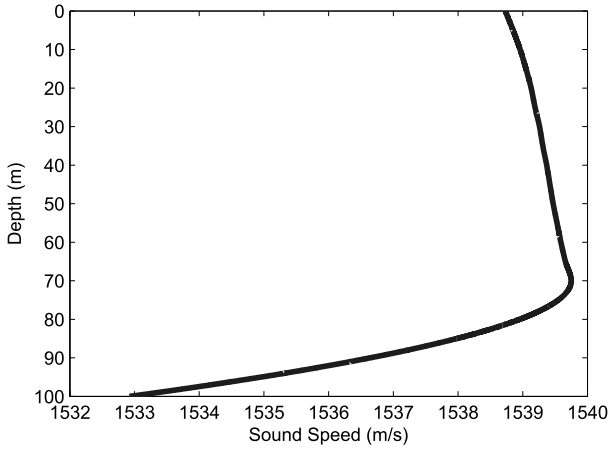

Figure 8: SSP of the scenario.

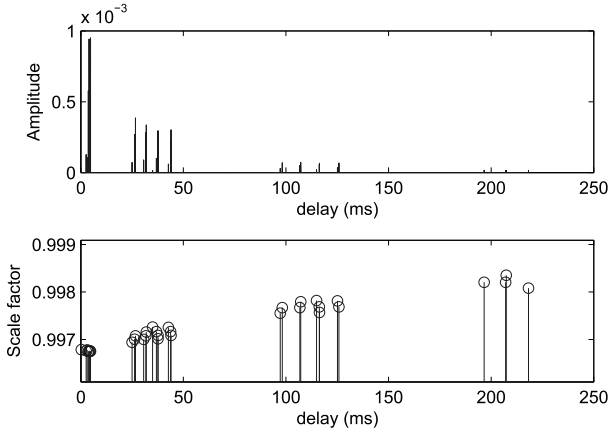

Figure 9: The amplitude and Doppler scale versus path delay at position $(400, 20)$.

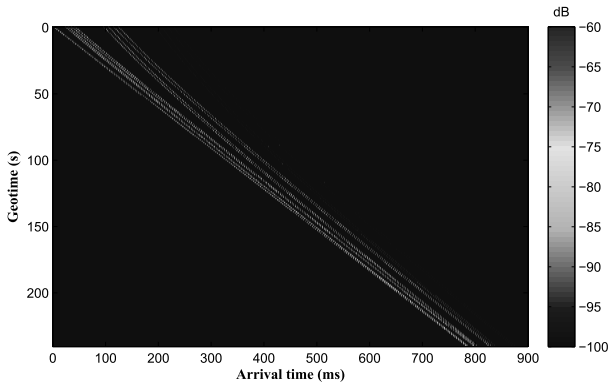

Figure 10: The time-varying CIR over 240s.

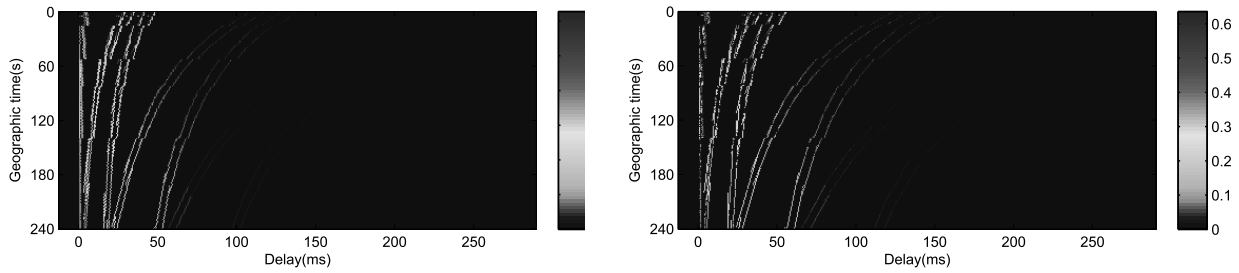

(a) Original time-varying CIR (b) Estimated time-varying CIR

Figure 11: Time-varying CIR and its estimate for the silence surface at SNR=0dB.

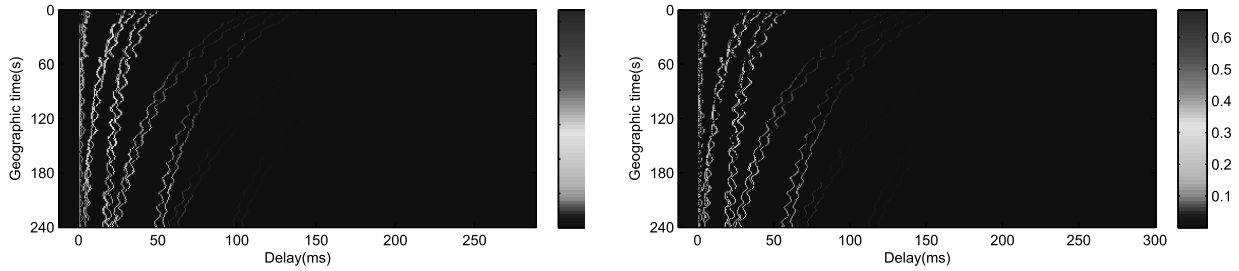

(a) Original time-varying CIR (b) Estimated time-varying CIR

Figure 12: Time-varying CIR and its estimate for the sinusoid surface at SNR=0dB.

The original time-varying CIR and its estimation by the proposed method at SNR=0dB, are shown in Fig.11. Note that for each geographic time, we normalize the amplitudes along the delay axis, and standardize the first arrival delay as 0ms.

Further, let us consider the case for a slightly complicated environment with a moving surface. Sometimes the surface motion is reasonable to modeled to move up and down vertically and the displacement varies sinusoidally in time [3] [7]. Thus, we consider a slow sinusoidally fluctuating surface with the sinusoid amplitude 2m and frequency 0.0625Hz, and estimate the time-varying parameters under the same condition as in the silence surface case. The original CIR and the its estimation at SNR=0dB are shown in Fig.12.

From Fig.11 and Fig.12, we can see that the proposed method can estimate the parameters of the dominant paths very well. This proves that the method can capture the time-varying property of the channel under noisy environment.

5. CONCLUSIONS

In the UWA applications, the relative motion can cause serious Doppler effect. Like the amplitudes and time delays, the Doppler scale factors of the multipaths are time-varying, which makes the channels more complicated. A parameter estimation method based on FRFT, for the wideband time-varying UWA channels, is proposed in this paper. It simplifies the receiver structure since extra hardware cost and storage are not required. Through simulation, we proves that the proposed method can obtain better performance than the single resampling method and the MP decomposition method, and is able to capture the time-varying property of the UWA channels under noisy environment.

6. REFERENCES

[1] M. Stojanovic and J. Preisig. Underwater acoustic communication channels: Propagation models and statistical characterization. *IEEE Communications Magazine*, 47(1):84–89, January 2009.

[2] T.H. Eggen, A.B. Baggeroer, and J.C. Preisig. Communication over doppler spread channels. part i: Channel and receiver presentation. *Oceanic Engineering, IEEE Journal of*, 25(1):62–71, Jan 2000.

[3] Chunshan Liu, Y.V. Zakharov, and Teyan Chen. Doubly selective underwater acoustic channel model for a moving transmitter/receiver. *Vehicular Technology, IEEE Transactions on*, 61(3):938–950, March 2012.

[4] Wen Xu, Tian Zhou, and Huifang Chen. A new approach for time reversal communication over doubly spread channels. In *Proceedings of the International Conference on Underwater Networks & Systems*, WUWNET '14, Rome, Italy, pages 7:1–7:8. ACM, 2014.

[5] Franz Hlawatsch and Gerald Matz. *Wireless Communications over Rapidly Time-Varying Channels*. Elsevier Ltd., 2011.

[6] P.A. van Walree and R. Otnes. Ultrawideband underwater acoustic communication channels. *IEEE Journal of Oceanic Engineering*, 38(4):678–688, Oct 2013.

[7] Parastoo Qarabaqi and Milica Stojanovic. Statistical characterization and computationally efficient modeling of a class of underwater acoustic communication channels. *IEEE Journal of Oceanic Engineering*, 38(4):701–717, 2013.

[8] L. Cannelli, G. Leus, H. Dol, and P. van Walree.

Adaptive turbo equalization for underwater acoustic communication. In *OCEANS - Bergen, 2013 MTS/IEEE*, pages 1–9, June 2013.

[9] Nicolas F Josso, Jun Jason Zhang, and et al. On the characterization of time-scale underwater acoustic signals using matching pursuit decomposition. In *OCEANS 2009, MTS/IEEE Biloxi-Marine Technology for Our Future: Global and Local Challenges*, pages 1–6. IEEE, 2009.

[10] Yanbo Zhao, Hua Yu, and Gang Wei. On the estimation of underwater acoustic channel delay-scale spreading function. In *Proceedings of the International Conference on Underwater Networks & Systems*, WUWNET '14, Rome, Italy, pages 36:1–36:2. ACM, 2014.

[11] Martin Siderius and Michael B. Porter. Modeling broadband ocean acoustic transmissions with time-varying sea surfaces. *The Journal of the Acoustical Society of America*, 124(1):137–150, 2008.

[12] J.R. Apel, M. Badiey, Ching-Sang Chiu, S. Finette, R. Headrick, J. Kemp, J.F. Lynch, A. Newhall, M.H. Orr, B.H. Pasewark, D. Tielbuerger, A. Turgut, K. von der Heydt, and S. Wolf. An overview of the 1995 swarm shallow-water internal wave acoustic scattering experiment. *Oceanic Engineering, IEEE Journal of*, 22(3):465–500, Jul 1997.

[13] Kenneth V. Mackenzie. Nine-term equation for sound speed in the oceans. *The Journal of the Acoustical Society of America*, 70(3):807–812, 1981.

[14] S.F. Mason, C.R. Berger, Shengli Zhou, and P. Willett. Detection, synchronization, and doppler scale estimation with multicarrier waveforms in underwater acoustic communication. *IEEE Journal on Selected Areas in Communications*, 26(9):1638–1649, December 2008.

[15] C.R. Berger, Shengli Zhou, J.C. Preisig, and P. Willett. Sparse channel estimation for multicarrier underwater acoustic communication: From subspace methods to compressed sensing. *IEEE Transactions on Signal Processing*, 58(3):1708–1721, March 2010.

[16] Srinivas Yerramalli and Urbashi Mitra. Optimal resampling of ofdm signals for multiscale–multilag underwater acoustic channels. *IEEE Journal of Oceanic Engineering*, 36(1):126–138, 2011.

[17] Ye Jiang and Antonia Papandreou-Suppappola. Discrete time-scale characterization of wideband time-varying systems. *IEEE Transactions on Signal Processing*, 54(4):1364–1375, 2006.

[18] Solomon W Golomb and Guang Gong. *Signal design for good correlation: for wireless communication, cryptography, and radar*. Cambridge University Press, 2005.

[19] Hans-Jurgen Zepernick and Adolf Finger. *Pseudo random signal processing: theory and application*. John Wiley & Sons, 2013.

[20] Xiufeng Song, P. Willett, and Shengli Zhou. Range bias modeling for hyperbolic-frequency-modulated waveforms in target tracking. *Oceanic Engineering, IEEE Journal of*, 37(4):670–679, Oct 2012.

[21] A.W. Rihaczek. Doppler-tolerant signal waveforms. *Proceedings of the IEEE*, 54(6):849–857, June 1966.

[22] VICTOR NAMIAS. The fractional order fourier transform and its application to quantum mechanics. *IMA Journal of Applied Mathematics*, 25(3):241–265, 1980.

[23] L.B. Almeida. The fractional fourier transform and time-frequency representations. *IEEE Transactions on Signal Processing*, 42(11):3084–3091, Nov 1994.

[24] Binbin Cheng, Hai Zhang, Jing Xu, and Gaodi Tang. Bat echolocation signal processing based on fractional fourier transform. In *Radar, 2008 International Conference on*, pages 460–463, Sept 2008.

[25] Liying Zheng and Daming Shi. Maximum amplitude method for estimating compact fractional fourier domain. *IEEE Signal Processing Letters*, 17(3):293–296, March 2010.

[26] L.G. Weiss. Wavelets and wideband correlation processing. *IEEE Signal Processing Magazine*, 11(1):13–32, Jan 1994.

[27] L.B. Almeida. The fractional fourier transform and time-frequency representations. *IEEE Transactions on Signal Processing*, 42(11):3084–3091, Nov 1994.

[28] Chris Capus and Keith Brown. Short-time fractional fourier methods for the time-frequency representation of chirp signals. *The Journal of the Acoustical Society of America*, 113(6):3253–3263, 2003.

[29] H.M. Ozaktas, O. Arikan, M.A. Kutay, and G. Bozdagt. Digital computation of the fractional fourier transform. *IEEE Transactions on Signal Processing*, 44(9):2141–2150, Sep 1996.

[30] J. Peterson, M. Porter, and M. Siderius. Virtual timeseries experiment code.